

## Advances in laser assisted 3D atom probe and its applications to light metals

K. Hono<sup>1,2</sup>, K. Oh-ishi<sup>1</sup>, C. L. Mendis<sup>1</sup>, and T. Ohkubo<sup>1,2</sup>

<sup>1</sup>National Institute for Materials Sciences, 1-2-1 Sengen, Tsukuba 305-0047, Japan

<sup>2</sup>CREST, Japan Science and Technology Agency, Japan

We review the recent advances in laser assisted 3D atom probe, which have facilitated the atom probe analysis of various materials including insulator oxides, and show typical atom probe results on the microalloying effects in aluminum and magnesium alloys.

**Keywords:** *Atom probe, solute clusters, precipitates, microalloying, aluminum alloys, magnesium alloys*

### 1. Introduction

The three dimensional atom probe (3DAP) is the only tomography technique with an atomic resolution. Due this unique feature, it has been widely used in semi-quantitative compositional analyses of solute clusters and nanosized precipitates in alloys. Various microalloying effects in the precipitation processes of aluminum alloys have been investigated using the 3DAP. The most well-known example is the effect of trace additions of Ag and Mg in Al-Cu based alloys [1]. In this system, Ag and Mg form co-clusters in the early stage of aging, which incorporate Cu to form {111} plates. As they grow, Ag and Mg segregate to the interface between the {111} precipitate denoted as  $\Omega$  and the  $\alpha$ -Al matrix, which reduces the strain energy at the interface. From the earliest stage of the solute clustering to the coarsening stage of the  $\Omega$ , the distribution of all solute atoms were visually monitored by the atom probe tomography [1]. While the combined addition of Mg and Ag leads to the formation of co-clusters, the microalloyed elements such as Sn and In are known to form fine precipitates that act as heterogeneous nucleation sites for the {001}  $\theta''$  plates [2].

Recently, the microalloying effects have also been recognized as one of the effective methods to enhance the age hardening processes in many magnesium alloys, [3]. Although magnesium alloys had not received serious attention as structural materials except in cast products, the attention towards the use of wrought magnesium alloys as the lightest structural metal for the weight reduction of automobiles and high speed trains has been increasing due to the ever increasing demand for carbon dioxide reduction in the transportation sector. The major obstacle against the use of Mg alloys as a structural component is the lack of wrought alloys that have competitive mechanical properties, formability and corrosion resistance with those of wrought Al alloys. The development of commercially viable low-cost, high strength wrought Mg alloys may expand the application areas of Mg alloys significantly considering that only a very small amount of Mg alloys is currently used as wrought products. Although rare earth containing Mg alloys are known to show pronounced age hardening [4], the application areas of rare earth containing alloys is rather limited due to the cost of materials. Thus, rare earth free alloys that exhibit pronounced age hardening effect must be sought for wider industrial applications.

The yield strengths of conventional commercial wrought Mg alloys such as Mg-Al based AZ31 and AZ61 and Mg-Zn based ZK60 are only about  $\sim 240$  MPa, which is less than 2/3 of that of wrought Al alloys. Commercial wrought Mg alloys have rarely been strengthened by precipitation although most of them are age hardening systems in view of phase equilibrium. Since most of the wrought Mg alloys are strengthened by the refinement of the crystal grain size that occurs during dynamic recrystallization in extrusion processes, subsequent artificial aging usually leads to a degradation of strength. However, if the age hardening response of an Mg alloy can be substantially enhanced to surpass the softening with the T6 or T5 treatment, the Mg alloy may also be precipitation hardened after the wrought processes like many Al wrought alloys. Our goal is to explore new Mg

alloys that can be solution treated before the wrought processes, and thereafter can be age hardened. To develop such alloys, it is essential to achieve pronounced age hardening responses that surpass the softening by recrystallization during subsequent artificial aging (T5 or T6). The enhancement of age hardening responses by microalloying and two-step aging have been used in a variety of Al alloys for many years; therefore, many insights should be obtained from the microalloying effects of Al alloys.

The three dimensional atom probe (3DAP) technique has been demonstrated to be useful for studying the microalloying effect in Al alloys [5]. The same approach should be possible for studying the microalloying effects in Mg alloys. However, very little atom probe work had been done on magnesium alloys until recently, mainly due to the difficulty of specimen preparation by the electropolishing technique and the frequent occurrence of specimen ruptures under the high electric field. In this paper, we review the recent advances in the laser assisted 3D atom probe, which have facilitated the atom probe analysis of various materials including insulator oxides in a revolutionary way, and show typical atom probe results on the microalloying effects in magnesium alloys.

## 2. Laser assisted 3D atom probe

The three-dimensional (3D) atom probe technique is now widely used to obtain the atomic tomography of metals and semiconductors [6]. To perform atom probe tomography, atoms on needle like specimens of a few 100 nm diameter must be field evaporated under the presence of an ultrahigh electric field of a few  $10^{10}$  V/m. In the conventional atom probe, such field evaporation was triggered by the application of ns voltage pulses ranging from 1 to 2 kV superimposed on high standing DC voltage typically ranging from 5 to 20 kV. The presence of the projection field from the tip to the detector results in a magnification of a few million by the projection effect. Since the conduction of the voltage pulse was not possible in insulating materials, the atom probe technique has been limited to conductive materials, mainly metals. Recent successful implementation of the pulsed laser to assist field evaporation [7,8] has expanded the application areas of the atom probe technique to a wider variety of materials including semiconductors [9] and thin film oxides [10,11]. In addition, the development of a site specific specimen preparation method using the focused ion beam technique [12] has broadened the application areas of the atom probe technique to magnetic multi-layers [13] and semiconductor devices [9]. The substantially reduced frequency of specimen ruptures in the pulsed laser assisted mode has also led to a practical analysis of these specimens. We have recently demonstrated that even bulk insulator ceramics can be analyzed with the 3DAP if the field evaporation of atoms is assisted with a short wave length (ultraviolet) ultrafast pulse laser [14]. A femtosecond Yb: KGd(WO<sub>4</sub>)<sub>2</sub> laser (Amplitude Systemes s-pulse (HR)) with third and fourth harmonic generators ( $\lambda=343$  nm and 257 nm, pulse duration of 400 fs) operating at a pulse frequency of 2 kHz or 100 kHz was adopted to a locally built straight type 3DAP instrument with CAMECA's fast delay line detector[3] as shown in Fig. 2. The flight length was 130 mm and the acceptance angle of the delay line detector was approximately 0.3 str. The laser beam was focused onto a spot size of approximately 150  $\mu$ m, which was irradiated to a tip apex from the side of the long axis. Although not much atom probe work had been done on Mg alloy until recently, we found that the application of UV femtosecond later to assist field evaporation facilitates the atom probe analysis of most magnesium alloys.

## 3. Microalloying Effect

The addition of trace elements to enhance the age hardening responses has already been proven in

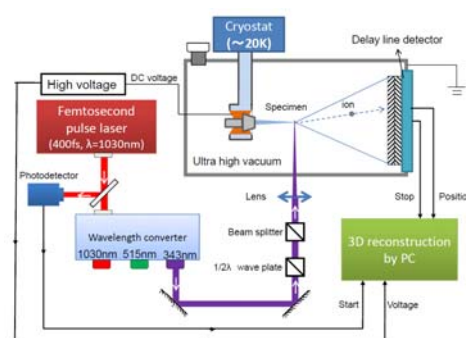


Fig. 1 Schematic illustration of the laser assisted 3D atom probe.

many age hardenable Al alloys, thus it is a realistic approach for Mg alloys as well. However, there has not been much investigation on the effectiveness of microalloying in Mg alloys. Recently, several investigations were carried out to enhance the age hardening responses of wrought Mg alloys.

The Mg-Zn system only showed a small precipitation hardening response [15]. Although previous investigations on the effect of 0.1at%Au [16], 0.1at%Ca [17] and 0.7at%Ag [18] additions to the Mg-Zn system did not report the enhancement of age hardening, we have recently found that the age hardening is substantially enhanced by the trace addition of 0.1at% Ag and a combined addition of 0.1at%Ag + 0.1at% Ca [19]. These elements were chosen due to the negative enthalpy of mixing between Zn and each of the trace elements, expecting Ag, Ca and Zn to cluster together to form preferential sites for the nucleation of the  $MgZn_2$  phase. Figure 1 shows the age hardening response of Mg-2.4at%Zn alloys with the addition of Ag, Ca, and Ag+Ca at 160°C.

The hardness increase of the microalloyed sample was more than two times higher than that of the Mg-2.4Zn binary alloy. Transmission electron microscopy (TEM) images of the Mg-2.4Zn, and Mg-2.4Zn-0.1Ag-0.1Ca alloys (Fig. 2) show that the size of the rod-like particles was significantly refined with the addition of Ag+Ca. The morphology and the crystal structure of the rod-like precipitates, which were identified as the  $MgZn_2$  phase, did not change with the Ag+Ca. However, the number density of the precipitates in the Ag+Ca containing alloy was found to be two orders of magnitude higher than that of the binary alloy, which accounted for the increased hardness.

The three-dimensional atom probe (3DAP) analysis results of the under-aged and peak-aged samples in Fig. 2 (c-d) suggest that the clusters of Ca and Zn were present in the under-aged sample, which are thought to act as nucleation sites for the subsequent precipitation of the  $MgZn_2$  phase [20], in which Ag and Ca atoms are enriched. (d) is an enlargement (c). [19]

The three-dimensional atom probe (3DAP) analysis results of the under-aged and peak-aged samples in Fig. 2 (c-d) suggest that the clusters of Ca and Zn were present in the under-aged sample, which are thought to act as nucleation sites for the subsequent precipitation of the  $MgZn_2$  phase [20], in which Ag and Ca atoms are enriched.

The Mg-2.4Zn-0.1Ag-0.1Ca-0.16Zr (at%) alloy showed a tensile yield strength of 290MPa with an elongation to failure at 17% after extrusion at 350°C as shown in Fig. 3. This high strength was partly due to the fine grain size that was formed by the dynamic recrystallization and precipitation during extrusion [21]. On aging at 160°C after the solution treatment (T6), the yield strength increased to 325MPa with an elongation to failure of 15%. The tensile strength of this alloy is comparable to that of the 5000 series Al alloys [20]; therefore, the specific strength is 1.6 times higher than that of 5000 Al. In addition, the compression/tension yield ratio for the as extruded alloy was approximately 0.9, much higher than that observed for the typical wrought Mg alloys (0.3-0.6). Through a series of work, we found

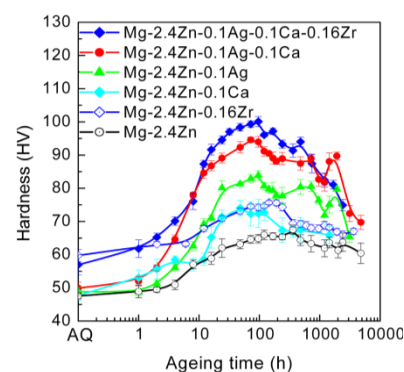


Fig. 2. The age hardening response of the Mg-Zn(-Zr) alloy with trace amounts of Ag and Ca. Reproduced from reference [19].

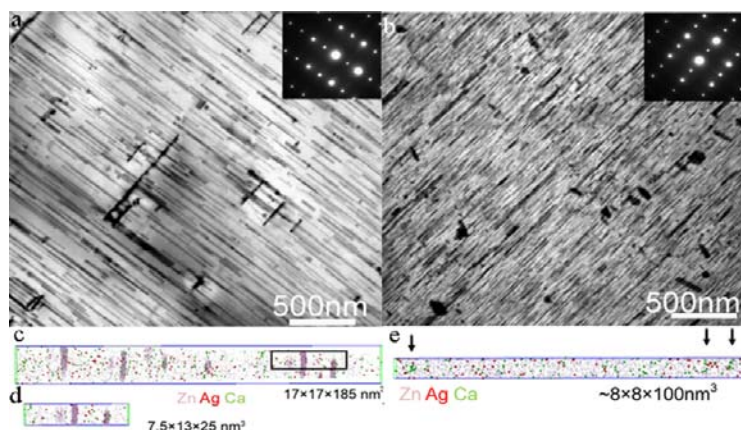


Fig. 3. Bright-field TEM micrographs of (a) Mg-2.4Zn and (b) Mg-2.4Zn-0.1Ag-0.1Ca. 3DAP data for Mg-2.4Zn-0.1Ag-0.1Ca (c-d) peak aged (e) 2h at 160°C (arrows indicate the clusters of Ca and Zn). (d) is an enlargement (c). [19]

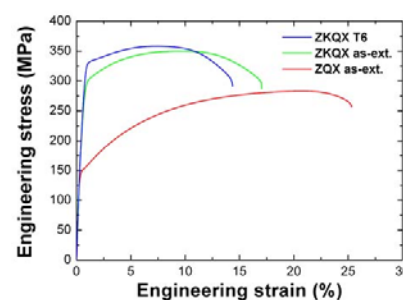


Figure 4 Tensile stress-strain curves of Mg-2.4Zn-0.1Ag-0.1Ca(-0.16Zr) alloys in as extruded and T6 treated states. [21]

that the precipitation of nano-sized particles by T6 aging resulted in a substantial increase in yield strength.

#### 4. Two-step aging

The classical nucleation theory suggests that the number density of nucleation sites increases as the supercooling increases. However, the precipitation kinetics also decreases at low temperature, thus the time to reach peak hardness increases. One way to overcome the long peak aging times while maintaining the fine dispersion of precipitates is to age at a lower temperature to introduce nucleation sites for precipitation and thereafter to carry out the 2nd stage aging at an elevated temperature. This double aging is commonly used in the 6000 series of Al alloys, and it has been a subject of many atom probe investigations [22]. However, double aging has not been widely used for Mg alloys.

A clear demonstration of the effectiveness of the double aging in the Mg alloy was made by the Mg-2.3Zn-2.8Al-0.5Mn (at%) alloys [23]. The age hardening curves in Fig. 4 show that the hardness of the double aged sample is significantly higher than that of the directly aged alloy. The number density of precipitates is increased substantially by double aging; the particle size has been refined drastically compared to that of the directly aged alloy as shown in the figure. The 3DAP result of the preaged alloy shows that the spherical G.P. zones are dispersed homogeneously. The extruded Mg-2.3Zn-2.8Al-0.5Mn alloy has tensile properties that are higher than those reported for the benchmark wrought magnesium alloy ZK60 following the duplex aging treatment [23].

#### 5. Guinier-Preston Zones

The Mg-Ca system also shows significant potential to precipitation hardening with a Mg<sub>2</sub>Ca phase having a high melting temperature of 711°C. The addition of Zn to Mg-Ca alloys was shown to result in the enhancement of the age hardening response [24-26] due to the formation of a large number density of single layer ordered Guinier Preston (G.P.) zones [25,26]. Similar GP zones were reported in Mg-RE-Zn alloys [27], and this is thought to be due to the large negative enthalpy of mixing between the

oversized atoms such as Ca (or RE) and the undersized Zn atoms. In cast and heat treated Mg-Ca-Zn alloys with similar compositions, the creep properties have been shown to be superior to those of the AZ91 alloy [28]. Therefore, Mg-0.3Ca-0.6Zn alloys have potential to be developed as a high strength creep resistant alloy with a careful choice of microalloying additions.

#### 5. Summary

The 3D atom probe has been widely used to investigate the solute clustering and precipitation

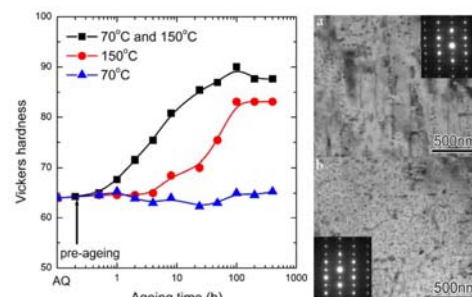


Fig. 5 Age hardening curve of the Mg-2.3Zn-2.8Al-0.5Mn alloy (a) aged at 150°C and (b) two step aged with preaging at 70°C for 48 h [23].

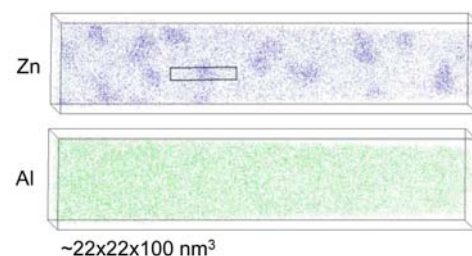


Fig. 5 Atom probe tomography of the Mg-2.3Zn-2.8Al-0.5Mn alloy preaged at 70°C for 48 h. [23]

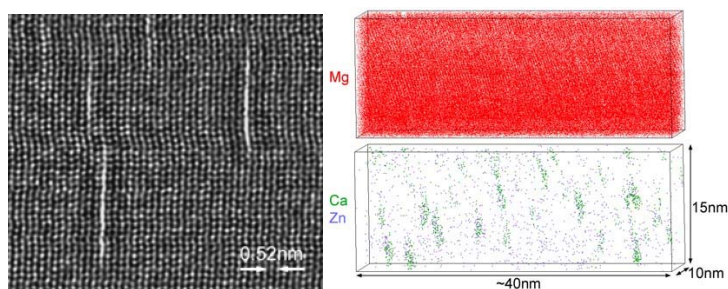


Fig.6 HAADF image of the peak aged Mg-0.3Ca-0.6Zn alloy and (b) atom probe tomography. [26]

processes of aluminum alloys; however, it had not been applied to magnesium alloys until recently. Recent implementation of ultrafast pulse laser to 3D atom probe has contributed in facilitating the atom probe analyses of magnesium alloys. We found that the UV femtosecond laser assisted atom probe field quantitative atom probe tomography of magnesium alloys and the microalloying effects in enhancing the age hardening responses of magnesium alloys have become subjects of atom probe investigations. We demonstrated that solute clustering and their interactions with nanosized precipitates in microalloyed wrought Mg alloys can be visualized using the atom probe tomography.

## Acknowledgment

This work was supported in part by the Ministry of Education, Science, Sports and Culture, Grant-in-Aid for Scientific Research (B), 21360348, 2009, and the World Premier International Research Center for Materials Nanoarchitectonics (MANA).

## References

- [1] L. Reich, M. Murayama and K. Hono, *Acta Mater.* 46 (1998) 6053.
- [2] H. K. Hardy, *J. Inst. Metals.* 78 (1950-51) 169.
- [3] K. Hono, C. L. Mendis, T. T. Sasaki, *Scripta Mater.* (2010), doi:10.1016/j.scriptamat.2010.01.038
- [4] T. Honma, T. Ohkubo, S. Kamado, K. Hono, *Acta Mater.* 55 (2007), 4137.
- [5] K. Hono, *Prog. Mater. Sci.* 47 (2002) 621.
- [6] M. K. Miller, *Atom probe tomography: analysis at the atomic level*, Kluwer Academic, New York, 2000.
- [7] B. Deconihout, F. Vurpillot, B. Gault, G. Da Costa, M. Bouet, A. Bostel, D. Blavette, A. Hideur, G. Martel and M. Brunel, *Surf. Interface Anal.* 39 (2007) 278.
- [8] B. Gault, F. Vurpillot, A. Bostel, A. Menand and B. Deconihout, *Appl. Phys. Lett.* 86, (2005) 094101.
- [9] T. F. Kelly, D. J. Larson, K. Thompson, R. L. Alvis, J. H. Bunton, J. D. Olson and B. P. Gorman, *Annu. Rev. Mater. Res.* 37 (2007) 681.
- [10] S. Pinitsoontorn, A. Cerezo, A. K. Petford-Long, D. Mauri, L. Folks and M. J. Carey, *Appl. Phys. Lett.* 93 (2008) 071901.
- [11] M. Kuduz, G. Schmitz and R. Kirchheim, *Ultramicroscopy*, 101 (2004) 197.
- [12] K. Thompson, D. J. Lawrence, D. J. Larson, J. D. Olson, T. F. Kelly and B. P. Gorman, *Ultramicroscopy* 107 (2007) 131.
- [13] D. J. Larson, A. K. Petford-Long, Y. Q. Ma, A. Cerezo, *Acta Mater.* 52 (2004) 2847.
- [14] Y. M. Chen, T. Ohkubo, M. Kodzuka, K. Morita and K. Hono, *Scripta Mater.* 61, 693 (2009).
- [15] G. Mima Y Tanaka *Trans. Jap. Inst. Met.* 12 (1971) 71.
- [16] E. O. Hall *J. Inst. Met.* 96 (1968) 21.
- [17] C. J. Bettles M.A. Gibson K. Venkatesan, *Scripta Mater* 51 (2004) 193.
- [18] S.C. Park J.D. Lim D. Eliezer, Shin, K.S. *Mater. Sci. Forum*, 419-422 (2003) 159.
- [19] C. L. Mendis K. Oh-ishi K. Hono, *Scripta Mater.* 57 (2007) 485.
- [20] C. L. Mendis K. Oh-ishi Y. Kawamura T. Honma S. Kamado K. Hono, *Acta Mater.* 57 (2009) 749.
- [21] K. Oh-ishi, C. L. Mendis, T. Honma, S. Kamado, T. Ohkubo, and K. Hono, *Acta Mater.* 57 (2009) 5593 .
- [22] M. Murayama and K. Hono, *Acta. Mater.* 47 (1999) 1537.
- [23] K. Oh-ishi, K. Hono, K.S. Shin, *Mater. Sci. Eng A* 496 (2008) 425.
- [24] J.F. Nie, B.C. Muddle *Scripta Mater* 37 (1997) 1475.
- [25] J. C. Oh, T. Ohkubo, T. Mukai, K. Hono *Scripta Mater.* 53 (2005) 675.

- [26] K. Oh-ishi, R. Watanabe, C.L. Mendis, K. Hono Mater. Sci. Eng. A 526 (2009) 177.
- [27] D. H. Ping, K. Hono, J.F. Nie, Scripta Mater. 48 (2003) 1017.
- [28] X. Gao, S. M. Zhu, B. C. Muddle, J. F. Nie Scripta Mater. 53 (2005) 1321